Optics Letters

On the Hamiltonian form of cross-mode modulation in nonlinear optical waveguides

Haofan Yang,[1] Weijin Chen,[1] Hanwen Hu,[1] Jing Xu,[1,2,*] Yuntian Chen,[1,2] and Xinliang Zhang[1,2]

[1]School of Optical and Electronic Information, Huazhong University of Science and Technology, Wuhan, China
[2]Wuhan National Laboratory for Optoelectronics, Huazhong University of Science and Technology, Wuhan, China
*Corresponding author: jing_xu@hust.edu.cn

Received 30 July 2018; revised 10 September 2018; accepted 10 September 2018; posted 11 September 2018 (Doc. ID 341005); published 9 October 2018

It is commonly believed that the Hamiltonian approach applies only to linear systems, or nonlinear systems with proper linearization procedures. In this Letter, we show that the Hamiltonian approach based on linear coupled-mode theory applies very well for cross-mode modulation, i.e., field variation of the probe light induced by a strong co-propagating pump light in a degenerate mode group. By deriving eigenvalues and eigenvectors of the nonlinear system, evolution of the probe light can be obtained, which agrees with numerical simulations of multimode nonlinear Schrödinger equations. Using the Hamiltonian approach, a simple approach for determining the pump mode for realizing arbitrary mode conversion is discussed. Two concrete scenarios of the optically induced vector mode conversions within the LP_{11}-mode group are further exemplified.

OCIS codes: (190.4370) Nonlinear optics, fibers; (060.2330) Fiber optics communications; (060.4370) Nonlinear optics, fibers.

https://doi.org/10.1364/OL.43.005005

Cross-mode modulation (XMM) is a nonlinear optical process that has received widespread attention in recent years [1–5], especially due to advances in spatial division multiplexing technologies in optical fiber communications [6]. In general, XMM manifests itself as an effect in which mode field distribution of a weak probe light changes over transmission when co-propagating with a much stronger pump light. Therefore, XMM offers an effective way to manipulate modal properties optically and dynamically, including the relative phase between different modes. Physically, the probe light can be decomposed into a series of eigenmodes that may experience different nonlinear phase shifts induced by the pump light. Mode field distribution of the probe light thus evolves in a manner similar to linear polarization rotation in a birefringent medium. In fact, such pump-induced birefringence has its form of nonlinear polarization rotation (NPR) in the single-mode scenario [7,8]. Horizontally polarized pump light introduces a slightly different propagation constant for electrical fields polarized horizontally and perpendicularly, as shown in Fig. 1(a). For an input probe light linearly polarized at 45°, the state of polarization is rotated by 90° at one-half of the beat length and recovered after transmission of a beat length, as shown in Fig. 1(b). XMM can be understood similarly. Figures 1(c) and 1(d) show the case in which the pump light is launched in the LP_{11}^{b} mode. Here LP_{11}^{a} (LP_{11}^{b}) refers to the LP_{11} mode with two lobes aligned vertically (horizontally). An input probe light also in the LP_{11} mode but with two lobes aligned at 45° can be equally split into the LP_{11}^{a} and LP_{11}^{b} modes, which experience different nonlinear propagation constants induced by the pump light. Therefore, mode field distribution of the probe light is rotated by 90° compared to the incident pattern over one-half of the beat length when the nonlinear phase shift imposed on the LP_{11}^{a} and LP_{11}^{b} mode is out of phase. The initial state is recovered after transmission of a beat length.

It is obvious that the prediction of the probe light depends on the selected modal basis. Therefore, the key to analysis of

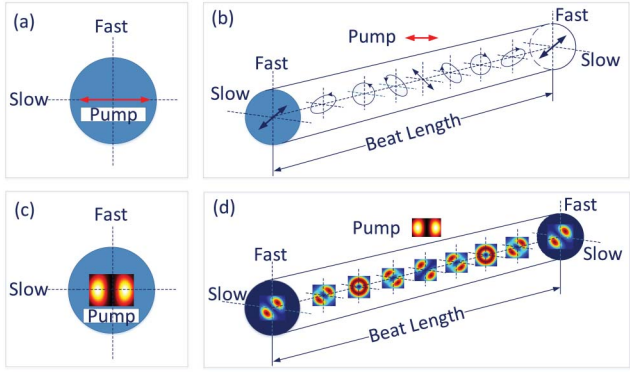

Fig. 1. (a) Nonlinear birefringence introduced by strong pump light launched in the fundamental mode and polarized horizontally. (b) Evolution of the state of polarization of a weak probe light linearly polarized at 45°. The fast and slow axes in (a) and (b) refer to the direction of polarization. (c) Nonlinear birefringence introduced by strong pump light at LP_{11}^{b} mode. (d) Evolution of mode field distribution of weak probe light launched into the LP_{11} mode with two lobes aligned at 45°. The probe light is co-polarized with the pump light in (d). The fast and slow axes in (c) and (d) refer to the direction in which the two lobes of the LP_{11} mode are aligned.

pump-induced birefringence is to find the proper modal basis of the system in the presence of the XMM's nonlinearity. Importantly, the impact of a given pump on the probe light in XMM can be treated as a linear effect in the typical pump–probe configuration, where the power of the pump light is much stronger than the probe light. In this Letter, we propose a linear mathematical framework, coined the Hamiltonian form, to derive the eigenstates and eigenvalues of the system in the presence of XMM nonlinearity based on the coupled-mode theory. The modal profiles of the probe light at different transmission distances are then readily obtained by calculating the linear superposition of eigenstates with nonlinear phase shifts.

We start from the Dirac notation of the Manakov equation for a modal group containing N degenerate modes [1], $\frac{\partial|E\rangle}{\partial z} = -\beta_1 \frac{\partial|E\rangle}{\partial t} - i\frac{\beta_2}{2}\frac{\partial^2|E\rangle}{\partial t^2} + i\gamma\kappa\langle E|E\rangle|E\rangle$, where the ket state $|E\rangle$ (see details in Ref. [1]), i.e., the modal contents of field amplitudes of the envelope, and β_1 and β_2 represent group delay per unit length and dispersion of group velocity, respectively. κ denotes random mode mixing [9], and γ is the nonlinear parameter [10]. In the pump–probe configuration, the total electrical field at the input of the nonlinear waveguide can be written as $|E\rangle = |a\rangle + |b\rangle$, where $|a\rangle/|b\rangle$ refers to the probe–pump light at wavelength λ_a/λ_b. Neglecting dispersion effects in the continuous-wave (CW) limit for both input lights, the components of $|E\rangle$ thus satisfy the following coupled equations:

$$\frac{\partial|a\rangle}{\partial z} = i\gamma\kappa(\langle b|b\rangle|a\rangle + |b\rangle\langle b|a\rangle), \tag{1a}$$

$$\frac{\partial|b\rangle}{\partial z} = i\gamma\kappa(\langle b|b\rangle|b\rangle), \tag{1b}$$

where the term $|b\rangle\langle b|a\rangle$ in Eq. (1a) accounts for the XMM, and $\langle b|$ is the conjugate transpose of $|b\rangle$. The four-wave mixing terms, i.e., $|b\rangle\langle a|b\rangle$ and $|a\rangle\langle b|a\rangle$ are dropped out, due to the lack of phase-matching condition in our system.

We first consider the simplest case, i.e., a two-mode coupling system. Equation (1b) is treated first by writing the pump light $|b\rangle$ as

$$|b\rangle = \sqrt{P_p}(p|\phi_1\rangle e^{i\zeta_{b1}z} + q|\phi_2\rangle e^{i\zeta_{b2}z}), \tag{2}$$

where P_p is the power of pump light, and ζ_{b1} and ζ_{b2} are nonlinear propagation constants induced by the self-phase modulation of the pump light itself. $|\phi_1\rangle$ and $|\phi_2\rangle$, satisfying orthonormal conditions given by $\langle\phi_i|\phi_j\rangle = \delta_{ij}(i,j=1,2)$, are eigenstates of the optical waveguides without pump-induced nonlinearity. p and q are normalized complex amplitude and satisfy $|p|^2 + |q|^2 = 1$. It is found that $\zeta_{b1} = \zeta_{b2} = \gamma\kappa P_p$ by inserting Eq. (2) into Eq. (1b). It is worthy to point out that the modal profile of the pump light $|b\rangle$ does not change over transmission, apart from the accumulated phase.

To find the eigenmodes of the coupled system given by Eq. (1a), the probe light $|a\rangle$ can be written as

$$|a\rangle = \sqrt{P_s}(m|\phi_1\rangle + n|\phi_2\rangle)e^{i\zeta z}, \tag{3}$$

where P_s is the power of the probe light, and eigenvalue ζ accounts for the nonlinear propagation constant induced by the pump light. m, n are normalized complex amplitude, satisfying $|m|^2 + |n|^2 = 1$. Inserting Eqs. (2) and (3) into Eq. (1a) and multipling with $\langle\phi_1|$ and $\langle\phi_2|$, the eigenvalue equation of the new system can be written as $H(mn)^T = \zeta(mn)^T$ by considering the orthonormality between modes. The Hamiltonian of the new system is given by

$$H = \gamma\kappa P_p\begin{pmatrix} |p|^2+1 & pq^* \\ qp^* & |q|^2+1 \end{pmatrix}. \tag{4}$$

The eigenvectors and eigenvalues are found to be

$$(m,n) = \{\{-q^*, p^*\}, \{p, q\}\}, \qquad \zeta = \gamma\kappa\{P_p, 2P_p\}. \tag{5}$$

Therefore, evolution of the probe light over transmission can be described by the following analytical expression:

$$|a\rangle = \sqrt{P_s}\sum_{i=1,2} a_i|\Phi_i\rangle e^{i\zeta_i L_{\text{eff}}}, \tag{6}$$

where $|\Phi_1\rangle = -q^*|\phi_1\rangle + p^*|\phi_2\rangle$ and $|\Phi_2\rangle = p|\phi_1\rangle + q|\phi_2\rangle$ are the two eigenmodes of the hybridized system, and a_i is the modal coefficient given by $a_i = \langle\Phi_i|a\rangle$. Evidently, $|\Phi_2\rangle$ is exactly the same pump mode, which means that the pump mode is always the eigenstates of the nonlinear system. The impact of transmission loss of the pump light can be taken into consideration by defining an effective length, i.e., $L_{\text{eff}} = (1 - e^{-\alpha L})/\alpha$, where α is the loss coefficient.

We proceed to discuss how to apply the above formalism to examine the mode rotation shown in Fig. 1(d), i.e., a system where two degenerate spatial modes with the same polarization is considered. To be more concrete, we consider a two-mode system with $|\phi_1\rangle/|\phi_2\rangle$, referred to as the normalized field of $\text{LP}_{11}^{a,x}/\text{LP}_{11}^{b,x}$. According to Fig. 1(d), $|a\rangle = |\phi_1\rangle$ and $|b\rangle = \frac{1}{\sqrt{2}}(|\phi_1\rangle + |\phi_2\rangle)$, i.e., $p = q = \frac{1}{\sqrt{2}}$, $m = 1$ and $n = 0$. The powers of the pump/probe light are 28 dBm/0 dBm, respectively. Superscript "x" represents x polarization. A step-index multimode fiber with a numerical aperture of 0.205 is considered in this work. The nonlinear coefficient of the fiber is $n_2 = 2.6\times10^{-20}$ m^2 W^{-1}, and the effective area of the fundamental mode is $A_{\text{eff}} \approx 43.7$ um^2. The corresponding γ is 2.41 W^{-1} km^{-1}, $\kappa \approx 0.76$. The attenuation coefficient of the fiber is $\alpha = 0.2$ dB/km. According to Eq. (5), the eigenvectors and eigenvalues of the new system are found to be $(m,n) = \frac{1}{\sqrt{2}}\{\{-1,1\},\{1,1\}\}, \zeta = \{1.156, 2.312\}\times10^{-3}$ rad/m, which means the eigenmodes of the coupled nonlinear system are LP_{11} modes with two lobes aligned either at 45° or −45°. The predicted power distribution in the $\text{LP}_{11}^{a,x}$ mode at wavelength λ_a over transmission distance is shown in Fig. 2 by the blue circles. It is seen that the mode profiles at local minimum points correspond to the $\text{LP}_{11}^{b,x}$ mode, and that there is a

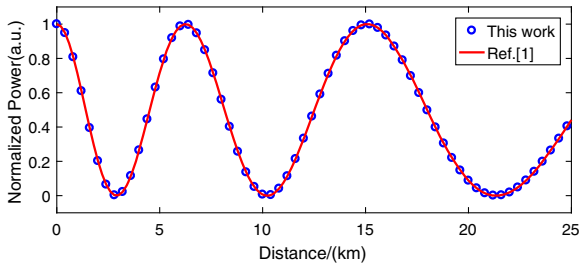

Fig. 2. Power distribution in the $\text{LP}_{11}^{a,x}$ mode at the probe light wavelength λ_a for a pump power of 28 dBm. The blue circles and red line are calculated by our method and by Ref. [1], respectively.

continuous exchange of energy between the $LP_{11}^{a,x}$ and $LP_{11}^{b,x}$ modes due to XMM-induced modal coupling. The increase in the oscillating period of the curves is due to transmission loss of the fiber. The result calculated according to Ref. [1] is shown by the red line in Fig. 2 for comparison, which is calculated by $\cos^2(\theta/2)$, where θ is the accumulated nonlinear phase shift defined according to Eq. (6) in [1]. It is clear that our method matches well with Ref. [1], which is further benchmarked against multimode nonlinear Schrödinger equations (MNLSE) [11].

Naturally, a more general question is that how to determine the pump mode for the transformation between a given input probe mode and a target output probe mode. It is well known that linear combinations of LP modes can generate vector modes. Therefore, a more general analysis of the XMM effects is necessary to predict the modal conversion between arbitrary vector modes. Without losing generality, we consider the case of the LP_{11} mode group with four degenerate modes. The pump light can be written as

$$|b\rangle = \sqrt{P_p}(p|\phi_1\rangle + q|\phi_2\rangle + u|\phi_3\rangle + v|\phi_4\rangle)e^{i\zeta_0 z}, \quad (7)$$

where $|\phi_1\rangle, |\phi_2\rangle, |\phi_3\rangle$, and $|\phi_4\rangle$ are eigenmodes of the optical waveguides without the pump light, and satisfy $\langle\phi_i|\phi_j\rangle = \delta_{ij}(i,j=1,2,3,4)$, and $|p|^2+|q|^2+|u|^2+|v|^2=1$. ζ_0 accounts for the nonlinear propagation constant. Similar to the two-mode situation, $|a\rangle$ can be written as

$$|a\rangle = \sqrt{P_s}(m|\phi_1\rangle + n|\phi_2\rangle + e|\phi_3\rangle + f|\phi_4\rangle)e^{i\zeta z}, \quad (8)$$

where m, n, e, f are normalized complex amplitude and satisfy $|m|^2 + |n|^2 + |e|^2 + |f|^2 = 1$. The Hamiltonian of the four-mode system is found to be

$$H = \gamma\kappa P_p \begin{pmatrix} |p|^2+1 & pq^* & pu^* & pv^* \\ qp^* & |q|^2+1 & qu^* & qv^* \\ up^* & uq^* & |u|^2+1 & uv^* \\ vp^* & vq^* & vu^* & |v|^2+1 \end{pmatrix}. \quad (9)$$

Eigenvalues ζ and corresponding eigenvectors at $p \neq 0$ are

$$\begin{aligned} \zeta &= \gamma\kappa\{P_p, P_p, P_p, 2P_p\}, \\ (m,n,e,f) &= \{\{-v^*,0,0,p^*\},\{-u^*,0,p^*,0\}, \\ &\quad \{-q^*,p^*,0,0\},\{p,q,u,v\}\}. \end{aligned} \quad (10)$$

For the other three cases, i.e., $q \neq 0, u \neq 0, v \neq 0$, expressions for the eigenvectors are different. For example, at $q \neq 0$, corresponding eigenvectors are

$$\begin{aligned} (m,n,e,f) &= \{\{0,-v^*,0,q^*\}, \\ &\quad \{0,-u^*,q^*,0\},\{q^*,-p^*,0,0\},\{p,q,u,v\}\}. \end{aligned} \quad (11)$$

The orthonormalized eigenvectors can be obtained after Gram–Schmidt orthogonalization. Note that the pump mode is always one of the eigenstates of the nonlinear system in the four-mode case, which is the same as the two-mode system. Another interesting feature is that the eigenvalue corresponding to the pump light mode is twice as large as that of the other eigenmodes, which is also true in the two-mode case.

Therefore, the four-mode system can be described in a similar way as a two-mode system in which the two modes are the pump mode as well as the sum of the other three eigenmodes, denoted by $|\psi_1\rangle$ and $|\psi_2\rangle$, respectively, after orthomormalization. The corresponding eigenvalues are ζ_1' and ζ_2', respectively. Thus, the required pump mode for converting an input probe mode into a target probe mode can be found by the following procedure. For the simplest case, we assume the input and output probe modes are the in-phase and out-of-phase addition of $|\psi_1\rangle$ and $|\psi_2\rangle$, respectively. That is, $|a\rangle = |\psi_1\rangle + |\psi_2\rangle e^{i\Delta\zeta z}$, where $\Delta\zeta = \zeta_2' - \zeta_1'$. The prefactor in front of $|a\rangle$ representing the power and phase is omitted for ease of reading. The probe light at the input and half beat length $d = \pi/|\Delta\zeta|$ can be written as $|a\rangle_{in} = |\psi_1\rangle + |\psi_2\rangle$ and $|a\rangle_{\text{out}} = |\psi_1\rangle - |\psi_2\rangle$, respectively. Therefore, $|\psi_1\rangle = |a\rangle_{in} + |a\rangle_{\text{out}}, |\psi_2\rangle = |a\rangle_{in} - |a\rangle_{\text{out}}$.

Now we study vector mode conversion in the LP_{11} mode group. Specifically, $|\phi_1\rangle, |\phi_2\rangle, |\phi_3\rangle$and$|\phi_4\rangle$ refer to the normalized field of $LP_{11}^{a,x}, LP_{11}^{b,x}, LP_{11}^{a,y}$ and $LP_{11}^{b,y}$, respectively. The vector modes TM_{01}, Even HE_{21}, TE_{01}, and Odd HE_{21} correspond to $\frac{1}{\sqrt{2}}(|\phi_2\rangle + |\phi_3\rangle)$, $\frac{1}{\sqrt{2}}(|\phi_2\rangle - |\phi_3\rangle)$, $\frac{1}{\sqrt{2}}(|\phi_1\rangle - |\phi_4\rangle)$, and $\frac{1}{\sqrt{2}}(|\phi_1\rangle + |\phi_4\rangle)$, respectively. Parameters are the same as in the two-mode case, except $\kappa = 0.61$. We target two different situations here, which convert the probe mode, i.e., TM_{01} as shown in Fig. 3(a), to the TE_{01} mode [Fig. 3(b), situation 1] and the Even HE_{21} [Fig. 3(c), situation 2], respectively. According to the theory of the four-mode system discussed above, the pump mode in situation 1 can be chosen as $TM_{01} + TE_{01}$ or $TM_{01} - TE_{01}$. The polarization and intensity distribution of $TM_{01} + TE_{01}$, i.e., $\frac{1}{2}(|\phi_1\rangle + |\phi_2\rangle + |\phi_3\rangle - |\phi_4\rangle)$, are shown in Figs. 3(d) and 3(e), respectively. Similarly, the pump light in situation 2 can be chosen as $TM_{01} +$ Even HE_{21} or $TM_{01} -$ Even HE_{21}. It can be easily shown that $TM_{01} +$ Even HE_{21} equals $|\phi_2\rangle$, as shown in Fig. 3(f). In the following, a plus sign is chosen for the pump mode of both situations. Table 1 shows eigenmodes and

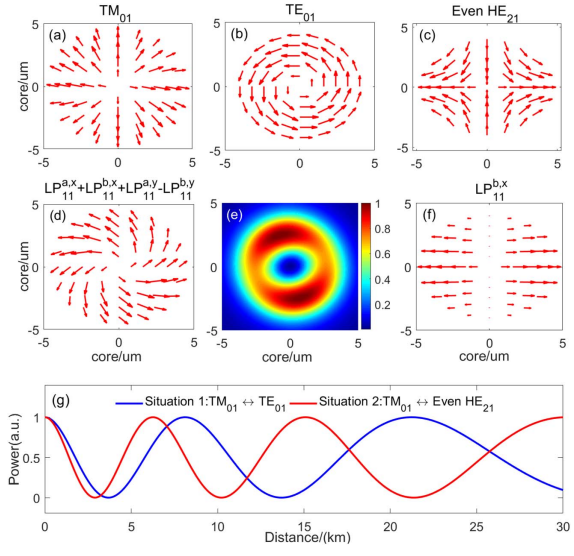

Fig. 3. Polarization/intensity distribution of the input probe mode (TM_{01}) (a); output probe mode at situation 1 (TE_{01}) (b) and situation 2 (Even HE_{21}) (c); pump mode at situation 1 ($LP_{11}^{a,x} + LP_{11}^{b,x} + LP_{11}^{a,y} - LP_{11}^{b,y}$) (d), (e) and situation 2 ($LP_{11}^{b,x}$) (f). (g) Power distribution in the TM_{01} mode at probe light wavelength λ_a versus propagation distance for two situations at a pump power of 28 dBm. The blue line and red line correspond to situations 1 and 2, respectively.

Table 1. Specific Parameters for Different Pump Modes of Signal Mode Conversion (Unit of ζ_i: 10^{-3} rad/m)

	Situation 1: TM_{01}↔TE_{01}	Situation 2: TM_{01}↔ Even HE_{21}
Pump mode	$\|b\rangle = \frac{1}{2}\sqrt{P_p}(\|\phi_1\rangle + \|\phi_2\rangle + \|\phi_3\rangle - \|\phi_4\rangle)e^{i\zeta_0 z}$	$\|b\rangle = \sqrt{P_p}\|\phi_2\rangle e^{i\zeta_0 z}$
$\|\Phi_i\rangle$	$\|\Phi_1\rangle = \frac{1}{2\sqrt{3}}(-\|\phi_1\rangle + 3\|\phi_2\rangle - \|\phi_3\rangle + \|\phi_4\rangle)$ $\|\Phi_2\rangle = \frac{1}{\sqrt{2}}(\|\phi_1\rangle + \|\phi_4\rangle)$ $\|\Phi_3\rangle = \frac{1}{\sqrt{6}}(-\|\phi_1\rangle + 2\|\phi_3\rangle + \|\phi_4\rangle)$ $\|\Phi_4\rangle = \frac{1}{2}(\|\phi_1\rangle + \|\phi_2\rangle + \|\phi_3\rangle - \|\phi_4\rangle)$	$\|\Phi_1\rangle = \|\phi_1\rangle$ $\|\Phi_2\rangle = \|\phi_4\rangle$ $\|\Phi_3\rangle = \|\phi_3\rangle$ $\|\Phi_4\rangle = \|\phi_2\rangle$
a_i	$a_1 = \frac{1}{\sqrt{6}}$ $a_2 = 0$ $a_3 = \frac{1}{\sqrt{3}}$ $a_4 = \frac{1}{\sqrt{2}}$	$a_1 = a_2 = 0$ $a_3 = \sqrt{\frac{1}{2}}$ $a_4 = \sqrt{\frac{1}{2}}$
ζ_i	$\zeta_1 = \zeta_2 = \zeta_3 = 0.928$ $\zeta_4 = 1.855$	$\zeta_1 = \zeta_2 = \zeta_3 = 1.156$ $\zeta_4 = 2.312$

eigenvalues calculated according to Eq. (10) or Eq. (11) for two situations. It can be seen that $|\Phi_4\rangle$ corresponds to the pump light mode in both situations 1 and 2, and the sum of the other three eigenmodes, i.e., $a_1|\Phi_1\rangle + a_2|\Phi_2\rangle + a_3|\Phi_3\rangle$, is equivalent to TM_{01} – TE_{01} and TM_{01} – Even HE_{21}, respectively, as expected. The predicted power distributions of the TM_{01} mode over transmission are shown in Fig. 3(g) for situations 1 (blue) and 2 (red), respectively, according to $|a\rangle = |\psi_1\rangle + |\psi_2\rangle e^{i\Delta\zeta z}$. It is the XMM-induced energy exchange between TM_{01} and TE_{01} (Even HE_{21}), given the normalized power oscillations between 0 and 1 in situation 1 (situation 2). The period of energy exchange of situation 2 is shorter than that of situation 1 due to the fact that $\Delta\zeta$ of situation 2 is larger than that of situation 1, according to Table 1.

Vector mode conversions within mode groups with degeneracy larger than four may exist in various scenarios, such as the LP_{21}/LP_{02} mode group in weakly guiding multimode fibers, LP11 mode group in multicore multimode fibers, etc. Multicore multimode fibers refer in particular to fibers with multiple cores sharing the same cladding and each core supporting multiple modes. Index differences between core and cladding are similar to conventional multi mode fibers to ensure a weakly guiding scenario. Higher-order degeneracy may happen by bringing the cores closer together [6]. For example, coupled three-core multimode fibers can support six degenerate fundamental modes, 12 degenerate LP_{11} modes, and 18 degenerate LP_{21}/LP_{02} modes. In general, vector mode conversions in a modal group of N-fold degeneracy can be described by expanding the pump light according to the N-degenerate mode set and deriving the Hamiltonian accordingly. Derivations show that the pump mode is always one of the eigenstates of the nonlinear system, and the eigenvalue corresponding to the pump light mode is twice as large as that of the other N-1 eigenmodes due to the strong symmetry of the Hamiltonian.

In conclusion, we show that the Hamiltonian approach can be applied very well for the XMM effect considered in a degenerate mode group in the pump–probe configuration. A simple analytical expression that describes the evolution of probe light can be obtained by deriving the eigenmodes and eigenvalues of the nonlinear system, and results agree with MNLSE simulations. It is shown that in both two-mode and four-mode cases, the pump mode is always the eigenstate of the nonlinear system, and the eigenvalue of the pump mode is twice as large as that of the other eigenmodes. Therefore, a four-mode system can be described in a similar way as a two-mode system. Finally, we discuss how to determine the required pump mode for the known input probe mode and target output probe mode, with two kinds of vector-mode conversion in the LP_{11} mode group considered. The linear approach can be further extended to simplify the analysis of mode groups with N-fold degeneracy ($N > 4$).

Funding. National Natural Science Foundation of China (NSFC) (61735006, 61775063); National Key Research and Development Program of China (2017YFA0305200).

REFERENCES

1. D. I. Kroushkov, G. Rademacher, and K. Petermann, Opt. Lett. **38**, 1642 (2013).
2. M. Schnack, T. Hellwig, and C. Fallnich, Opt. Lett. **41**, 5588 (2016).
3. R. J. Essiambre, M. A. Mestre, R. Ryf, A. H. Gnauck, R. W. Tkach, A. R. Chraplyvy, Y. Sun, X. Jiang, and R. Lingle, IEEE Photon. Technol. Lett. **25**, 535 (2013).
4. N. M. Lüpken, T. Hellwig, M. Schnack, J. P. Epping, K. J. Boller, and C. Fallnich, Opt. Lett. **43**, 1631 (2018).
5. Z. Pan, Y. Weng, and J. Wang, Photon. Netw. Commun. **31**, 305 (2016).
6. D. J. Richardson, J. M. Fini, and L. E. Nelson, Nat. Photonics **7**, 354 (2013).
7. K. Kitayama, Y. Kimura, K. Okamoto, and S. Seikai, Appl. Phys. Lett. **46**, 623 (1985).
8. M. Winter, C. A. Bunge, D. Setti, and K. Petermann, J. Lightwave Technol. **27**, 3739 (2009).
9. A. Mecozzi, C. Antonelli, and M. Shtaif, Opt. Express **20**, 11673 (2012).
10. G. P. Agrawal, *Nonlinear Fiber Optics*, 5th ed. (Academic, 2013).
11. F. Poletti and P. Horak, J. Opt. Soc. Am. B **25**, 1645 (2008).